SOIL COMPACTION

EFFECTS ON SOIL HYDRAULIC PROPERTIES AND PREFERENTIAL WATER FLOW

Mona Mossadeghi Björklund

Licentiate Thesis
Swedish University of Agricultural Sciences
Uppsala 2020

SOIL COMPACTION

EFFECTS ON SOIL HYDRAULIC PROPERTIES AND PREFERENTIAL WATER FLOW

Mona Mossadeghi Björklund
Swedish University of Agricultural Sciences
Department of Soil and Environment
Uppsala

SLU
SWEDISH UNIVERSITY OF AGRICULTURAL SCIENCES

Licentiate thesis
Swedish University of Agricultural Sciences
Uppsala 2020

Cover: Jokioinen, POSEIDON-NORDIC project
(photo: A, Simojoki)

Abstract

Soil compaction caused by passage of agricultural machinery over the surface is an issue in many agricultural soils with a high clay content. Compaction is known to modify soil pore structure and soil hydraulic properties, but can also affect the occurrence of preferential flow. Water flow through preferential flow pathways can facilitate transport of fertilisers, pesticides and contaminants to groundwater, creating harmful environmental problems. In two complementary studies, this thesis examined soil hydraulic properties and preferential water flow on soil cores sampled in the field and quantified flow patterns *in situ* at two sites approximately 300 m apart in central Sweden. One year after compaction of field plots, X-ray computed tomography (CT) imaging was used to visualise and quantify soil pore structures in soil columns taken from the subsoil (30-50 cm depth). Degree of preferential water flow and transport were derived from non-reactive tracer breakthrough curves. Dye tracing experiments were performed in the field and different soil mechanical and hydraulic properties were measured to help explain the dye patterns.

Contrasting effects of wheel traffic were observed at the two neighbouring sites. Thus, even quite small differences in initial soil and site conditions can significantly influence the extent to which applied compaction stresses affect the connectivity of structural pore space in soil and, consequently, water flow patterns. These results contradict previous findings of an increase in preferential flow following soil compaction. This discrepancy in results was analysed with the help of a conceptual model, which suggested that preferential flow is greatest at some intermediate level of compaction at which macropore continuity is still maintained, despite reductions in macroporosity. The model also illustrated how compaction, and subsequent recovery from compaction, might affect susceptibility to preferential flow and surface runoff. To prevent subsoil compaction, it is important to consider soil conditions at the time of trafficking, which can significantly influence the effect of compaction on soil pore connectivity and associated water flow.

Keywords: Subsoil compaction, air permeability, breakthrough curve, CT-imaging, penetration resistance, saturated hydraulic conductivity, dye tracing, macroporosity, soil pore structure, water flow

Author's address: Mona Mossadeghi Björklund, Department of Soil and Environment, SLU, P.O. Box 7014, 750 07 Uppsala, Sweden
E-mail: mona.mossadeghi@slu.se

Dedication

To my sons, Yosef and Yones.

Education is not the learning of facts, but the training of the mind to think.
Albert Einstein

Contents

List of Publications

This thesis is based on the work contained in the following papers, referred to by Roman numerals in the text:

I Mossadeghi-Björklund, M., Arvidsson, J., Keller ,T., Koestel, J., Lamandé, M., Larsbo, M. & Jarvis, N. 2016. Effects of subsoil compaction on hydraulic properties and preferential flow in a Swedish clay soil. *Soil & Tillage Research* 156: 91-98.

II Mossadeghi-Björklund, M., Jarvis, N., Larsbo, M., Forkman, J. & Keller, T. 2019. Effects of compaction on soil hydraulic properties, penetration resistance and water flow patterns at the soil profile scale. *Soil Use and Management* 35(3): 367-377.

The contribution of Mona Mossadeghi-Björklund to the papers included in this thesis was as follows:

I Performed the field and laboratory work and carried out data analysis with supervision from NJ, JA, TK, ML and JK. Mathieu Lamandé performed the CT image analyses. Designed the paper layout and did most of the writing.

II Performed the field and laboratory work and carried out data analysis with supervision from NJ, TK, ML and JK. Designed the paper layout and did most of the writing.

Abbreviations

Symbol	Definition
BTC	Breakthrough curve
K_s	Saturated hydraulic conductivity
K_a	Air permeability
$t_{0.05}$	5% arrival time
CT	Computed tomography

1 Introduction

1.1 Soil compaction

Soil compaction in a strict sense is the process by which bulk density increases and soil porosity decreases. Compaction may be caused by passage of agricultural machinery over the field and typically not only reduces pore volume, but also modifies pore connectivity and continuity and pore size distribution (Servadio *et al*., 2001). Previous studies suggest that compaction reduces the saturated and near-saturated hydraulic conductivity of soil (Arvidsson, 1997; Schwen *et al*., 2011) and increases the risk of surface runoff (Lipiec & Hatano, 2003). Compaction may also increase the probability of preferential flow in any remaining macropores (Kulli *et al*., 2003) or those that regenerate after compaction (Jarvis, 2007). This can facilitate transport of fertilisers, pesticides and pollutants to receiving water bodies and groundwater resources.

There is a difference between topsoil and subsoil compaction. Topsoil compaction refers to compaction within tillage depth (0-0.3 m) and is caused primarily by pressure applied to the soil surface. Freeze-thaw and wetting-drying cycles can help reverse topsoil compaction. The effects of topsoil compaction may also be partly reversed by mouldboard ploughing (Arvidsson & Håkansson, 1996), whereas the effects of subsoil compaction may be more persistent (Etana & Håkansson, 1994). Due to its persistence, subsoil compaction is a major concern for agricultural soils. Some field operations, such as deep subsoiling, can alleviate subsoil compaction, but the result is not always worth the costs (Chamen *et al*., 2015). Therefore, efforts should be made to minimise soil compaction due to its harmful effects on soil pores, and subsequent negative consequences for plant root growth and enhanced runoff and leaching of fertilisers and pesticides to groundwater (Kim *et al*., 2010).

1.2 Macropores and preferential flow

Macropores are large, continuous structural pores in soil and include shrinkage cracks, tillage fractures, root channels and soil fauna burrows. It has been suggested that pores larger than about 0.3-0.5 mm diameter, which are equivalent (assuming cylindrical pore shape) to pores that empty at water pressures of -10 to -6 cm, can be classified as macropores (Jarvis, 2007). They are important because they largely govern transport functions. Preferential flow refers to non-equilibrium flow where water and solutes move rapidly through the macropores and only interact with the soil matrix to a limited extent. Because of rapid water movement, preferential flow can lead to faster solute transport and affect groundwater quality by fertiliser and pesticide leaching (Vanclooster *et al*., 1995; Goulding *et al*., 2000).

In general, two conditions must be met for macropores to contribute to preferential flow. First, the macropore must be partly or completely filled with water and, second, the macropore must extend continuously over a significant portion of the porous medium (Hendrickx *et al*., 2001). A common example of preferential flow at pore scale is flow through earthworm burrows or root channels when a section of the soil matrix reaches saturation or at least is close to saturation. Water and chemicals can bypass the topsoil by travelling in such channels, and pollutants and pesticides can potentially contaminate shallow groundwater resources.

Although preferential flow is typically associated with flow through macropores, it can also occur at other scales, referred to as Darcian scale and areal scale (Hendrickx *et al*., 2001). At the Darcian scale, preferential flow may occur in homogeneous soils with no pronounced macropore structure, *e.g*. in soils where coarse-textured layers are overlain by less permeable layers or in soils with water-repellent zones. At the areal scale, surface depressions and discontinuous layers with lower or higher permeability can cause preferential flow. In this thesis work, the focus was on preferential flow at the pore to profile scale, *i.e*. predominantly preferential flow through macropores.

1.3 Methods to quantify the occurrence of preferential flow

Preferential flow is difficult to measure and quantify. One important reason for the limited progress to date in quantification of preferential flow is the difficulty in quantifying important pore system characteristics that control water flow and solute transport. Thus, evidence of preferential flow is often indirectly inferred from unexpectedly early water and chemical breakthrough or from unexpectedly deep water and chemical migration in soil. Today, there are many methods available to quantify macropore networks in soil, each with their own advantages

and disadvantages (Allaire *et al*., 2009). Dye tracer experiments and X-ray computed tomography (CT) techniques are the most commonly used approaches to characterise preferential flow through macropores. Dye tracer experiments provide qualitative pictures to illustrate the flow pathways in soil (Alaoui & Goetz, 2008) and dye tracing is generally a reliable technique for visualisation, identification and quantification of water flow pathways in structured soils (Janssen & Lennartz, 2008). Direct evidence of the presence of preferential flow can be obtained from dye tracer patterns (Hendrickx & Flury, 2001). However, dye tracer tests only provide information in two dimensions. They are also relatively work-intensive, requiring excavation of soil pits and preparation of soil profile walls.

In contrast, X-ray CT imaging is an effective non-destructive scanning method that can visualise and quantify soil pore structures in three dimensions (Kim *et al*., 2010; Lamandé *et al*., 2013; Larsbo *et al*., 2014). A CT image is a three-dimensional image of the inside of an object constructed from a large series of two-dimensional X-ray images taken around a single axis of rotation. Petrovic *et al*. (1982) were the first to apply CT imaging in soil science, with the aim of determining soil bulk density. Since their work, the use of CT imaging in soil science studies has increased greatly. The results have considerably improved understanding of how soil structure and pore connectivity influence water movement, particularly in soils where preferential flow is prevalent (Mooney, 2002). Computed tomography imaging can also be a very useful approach in studies targeting characterisation of soil pore modification after compaction (Pires, 2011). However, while CT imaging techniques have great potential, they also have severe drawbacks in terms of accessibility, resolution and artefacts (Mooney, 2002). For example, CT imaging is restricted to analysis of "isolated" soil cores, whereas dye tracing allows investigation of water flow within a whole soil profile (Wildenschild & Sheppard, 2013). Thus, sample size is one limitation of the technique. Therefore, in this thesis, both CT images and dye tracing patterns were used to gain a better understanding of the flow and transport properties in soil after compaction.

The degree of preferential flow can also be quantified in intact soil columns in breakthrough curve (BTC) experiments. In this method, a solution containing the chemical of interest is applied to one end of the soil column and its concentration is measured in the effluent at the other end of the column, under steady water flow. The relationship between the relative solute concentration in the effluent and time elapsed or amount of water passing through the soil column is called the breakthrough curve. The shape of the breakthrough curve is then analysed to study the function of the pore system in the transport process. From the shape of breakthrough curves, useful information such as the 5% arrival time

($t_{0.05}$), *i.e.* the time, relative to the average arrival time, for 5% of the applied tracer mass to arrive at the bottom of the sample, can be obtained. The $t_{0.05}$ value obtained can be used to deduce the presence of preferential flow (Koestel *et al*., 2011). It has been identified as a robust indicator of preferential transport, with smaller $t_{0.05}$ values indicating stronger preferential flow (Ghafoor *et al*., 2013; Knudby & Carrera, 2005; Koestel *et al*., 2011, 2012). In a study carried out on 733 tracer BTC experiments by Koestel *et al*. (2012), it was suggested that $t_{0.05}$ >0.5 indicates absence of preferential flow, while values <0.22 indicate strong preferential flow.

1.4 Compaction effects on the pore system and preferential flow

It is generally suggested that compaction results in a massive soil structure, through homogenisation of the pore system and creation of smaller pores (Servadio *et al*., 2001). The pore fractions most affected by compaction include macropores or coarse mesopores (Alaoui *et al*., 2011; Cassaro *et al*., 2011), which are vitally important for soil aeration and water transport. For example, Lipiec and Håkansson (2000) found that an increase in the number of vehicle-passes from zero to eight decreased macroporosity from 13.4% to 5.6%. Compaction not only modifies the pore volume, but also alters the connectivity and continuity of pores (Alaoui *et al*., 2011). Changes in the characteristics and geometry of structural pore networks following compaction can significantly influence the risk of rapid preferential solute transport in soil macropores (Hendrickx & Flury, 2001; Jarvis, 2007). As compaction mainly disrupts or destroys the larger pores in soil, it can be expected to reduce the strength of preferential flow, *e.g*. Heitman *et al*. (2007) observed slower breakthrough of non-reactive solute in compacted plots. On the other hand, some studies report strong preferential flow following compaction in macropores remaining after compaction, or macropores regenerated later due to physical or biological processes (Alaoui & Goetz, 2008; Kulli *et al*., 2003).

2 Thesis work

The aim of this thesis was to determine the effects of compaction on soil hydraulic properties and identify how this affects preferential flow in soil. To achieve this objective, two complementary studies (Papers I and II) were carried out at the same two experimental sites. Paper I focused on soil hydraulic properties and preferential water flow in soil columns sampled in the field, while Paper II involved *in situ* quantification of flow patterns. Both studies combined field and laboratory data from the same sites, to gain a better understanding of compaction effects on preferential flow.

2.1 Paper I: Compaction effects on preferential flow

Paper I examined the effects of compaction on preferential water flow in soil columns (20 cm in diameter, 20 cm height) taken from the subsoil (30-50 cm depth). X-ray computed tomography (CT) imaging was used to visualise and quantify soil pore structures in the soil columns. The degree of preferential water flow (5% arrival time, $t_{0.05}$) was calculated from non-reactive tracer breakthrough curves. Saturated hydraulic conductivity (K_s) and air permeability (K_a) at field moisture content were also measured. The soil macroporosity values derived from CT images were then related to air permeability, 5% arrival time and saturated hydraulic conductivity, to get a better understanding of pore system functioning. The hypothesis tested in Paper I was that soil compaction increases the presence of preferential flow.

2.2 Paper II: Compaction effects on flow patterns

In Paper II, the aim was to quantify the effects of compaction on water flow patterns at the soil profile scale. Because of the interaction between the natural recovery processes and induced compaction, quantifying soil compaction effects on water flow patterns is challenging, This complexity means that the impacts

of compaction on water flow patterns in agricultural soils are still poorly understood. One year after establishing the compaction treatment, dye tracing experiments were performed and a range of soil mechanical and hydraulic properties (*i.e.* penetration resistance, bulk density, macroporosity and mesoporosity) were measured, to help explain the dye patterns.

3 Materials and Methods

The same field experiments were used in Paper I and Paper II, and therefore the site description and experimental design are identical for both papers.

3.1 Site description and experimental design

The compaction experiments were carried out at two field sites (Upper and Lower, approximately 300 m apart) on a well-structured clay soil (45-54% clay) close to Uppsala in central Sweden. The groundwater level at the sites is regulated by a nearby stream and is approximately 50 cm higher at the Upper site than at the Lower site. Detailed information about the two sites can be found in Papers I and II. Some basic properties of the soils at the sites are presented in Table 1.

Table 1. *Soil texture and organic matter content of soils from the Upper and Lower experimental sites used in Papers I and II*

Site	Sampling depth	Particle size distribution (%)			Organic matter content (%)
		Clay (<0.002 mm)	Silt (0.002-0.06 mm)	Sand (0.06-2 mm)	
Upper	15 cm	47.3	31.5	21.2	3.5
	30 cm	46.5	32	21.5	1.3
	50 cm	46.5	35.3	18.2	0.3
Lower	15 cm	50	30	20	3
	30 cm	50.5	32.5	17	0.3
	50 cm	53.8	32.5	13.7	0

Two randomised complete block trials were designed, with two treatments (compacted and control), four blocks of two plots at each site and plot size 9 m × 20 m (Figure 1).

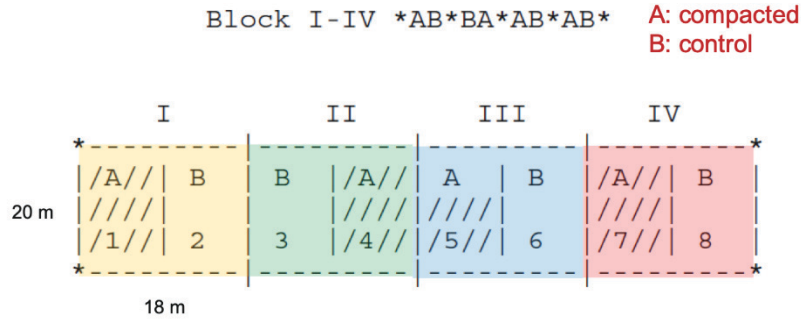

Figure 1. Randomized block design used at both the Upper and Lower sites, with four blocks (1-4) and two treatments (A, B) in eight plots (1-8).

The compaction treatment was performed by four passes with a three-axle dumper truck (Bell B25D 6×6) with 5.8, 5.4 and 4.6 Mg wheel load on the first, second and third axle and 420 kPa tyre inflation pressure (tyre size: 23.5R25) (Figure 2). After compaction, both sites were mouldboard ploughed to a depth of approximately 20 cm. An oat crop was grown at both sites, with seedbed preparation and sowing in spring and harvest at the end of August.

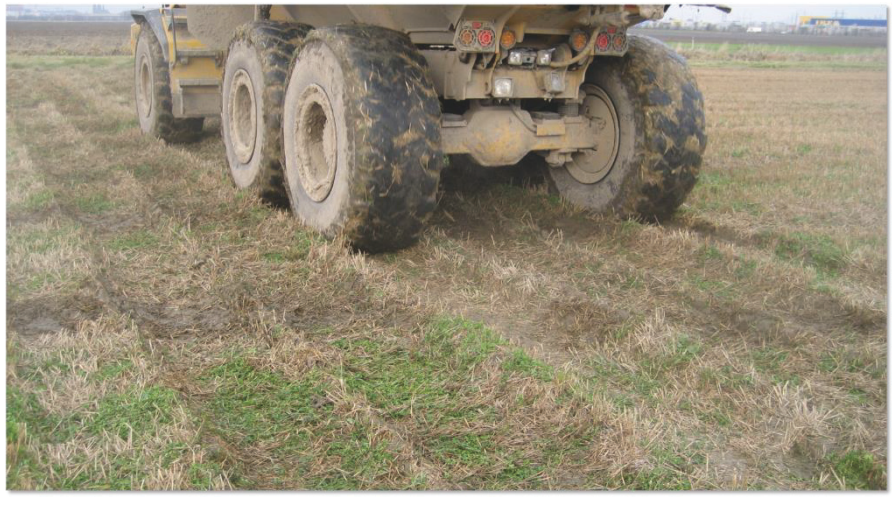

Figure 2. Experimental compaction treatment involving four passes with a 5-ton wheel load dumper truck.

One year after the compaction treatment, soil column/core sampling and field measurements were carried out, at a time when the soil was slightly wetter than field capacity.

3.2 Sampling

32 large soil columns (20 cm height, 20 cm diameter), were extracted from the 30-50 cm soil layer in compacted and control plots at the Upper and Lower sites (two per plot). After sampling, the soil columns were tightly closed at both ends to avoid evaporation and were stored at 1 °C to prevent earthworm activity until measurements. Before starting the laboratory measurements, the tops and bottoms of the soil columns were carefully trimmed with the point of knife to reveal undisturbed soil. These soil columns were used for CT imaging, solute breakthrough experiments and hydraulic conductivity measurements in Paper I.

For measurements in Paper II, in September 288 small soil cores (5 cm height, 7.2 cm diameter) were extracted from three depths (10, 30 and 50 cm) in compacted and control plots at the two sites (Figure 3).

Figure 3. Sampling of small soil cores (5 cm height, 7.2 cm diameter) in field plots.

On arrival at the laboratory sampling, the soil cores were gradually saturated from the base. Half of the soil cores (n=144) were used for measurements of

saturated hydraulic conductivity and the other half for water retention and bulk density measurements.

3.3 Computed tomography (CT) imaging (Paper I)

A medical CT scanner with pore resolution 1.2 mm diameter was used to produce CT images of the soil columns (Figure 4). Detailed information about the method and image analyses can be found in Paper I.

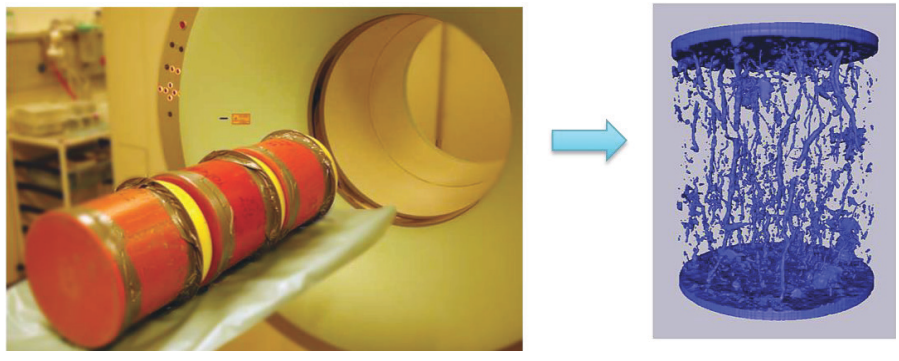

Figure 4. (Left) Use of a medical computed tomography (CT) scanner to visualise the pore system in soil columns and (right) example of a CT image. Photo by Mathieu Lamandé.

Macroporosity, connected porosity and total number of individual macropore clusters (no. of pores) were calculated from the CT images.

3.4 Solute breakthrough curve (BTC) (Paper I)

Solute breakthrough experiments on large soil columns from the Upper site were carried out in a laboratory irrigation chamber (constant rate, 5 mm h^{-1}). Because of very low hydraulic conductivity at the Lower site, the solute breakthrough experiment on those soil columns was carried out under ponding conditions (Figure 5). The electrical conductivity of the effluent was logged at 1-minute intervals using electrical conductivity meters, to provide breakthrough curves (BTCs). From these BTCs, the relative 5%-arrival time $t_{0.05}$ (-), was derived. Detailed information about the method and analyses can be found in Paper I.

Figure 5. Equipment used for breakthrough experiments under ponding conditions on soil columns from the Lower site (Paper I).

3.5 Saturated hydraulic conductivity (K_s) (Paper I)

The saturated hydraulic conductivity, K_s, of each column was measured using the falling-head method according to Jury *et al*. (1991), with an initial ponding height at the soil surface of 20 cm (Figure 6). Saturated hydraulic conductivity for the large columns was then calculated as:

$$Ks = \left(\frac{L}{t1}\right) Ln\,(\frac{b0 + L}{b1 + L})$$

where L is cylinder height (20 cm), $b0$ is initial water level (20 cm) and $b1$ is water level at time $t1$.

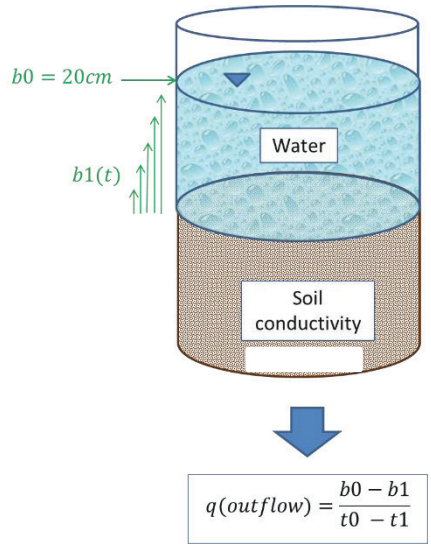

Figure 6. Schematic diagram of the falling head test used for measuring saturated hydraulic conductivity (K_s) on soil columns (Paper I).

3.6 Air permeability (K_a) (Paper I)

Air permeability (K_a) of the soil columns at field water content was measured using the method developed by Iversen *et al*. (2001). The volumetric air flow rate through the soil columns was recorded and the air permeability was then calculated from Darcy's law (Figure 7).

Air permeability is defined as the rate of airflow passing perpendicularly through a known area under a prescribed air pressure differential between the two surfaces of a material. It is calculated as:

$$K_a = \frac{q_v \times \mu \times L_s}{\rho \times g \times A_s \times h}$$

where K_a is air permeability (μm^2), q_v is air flow, μ is viscosity of air, g is acceleration due to gravity, ρ is density of water, L_s is sample height (in this case 20 cm), A_s is sample area and h is manometer reading (in this case 5 hPa).

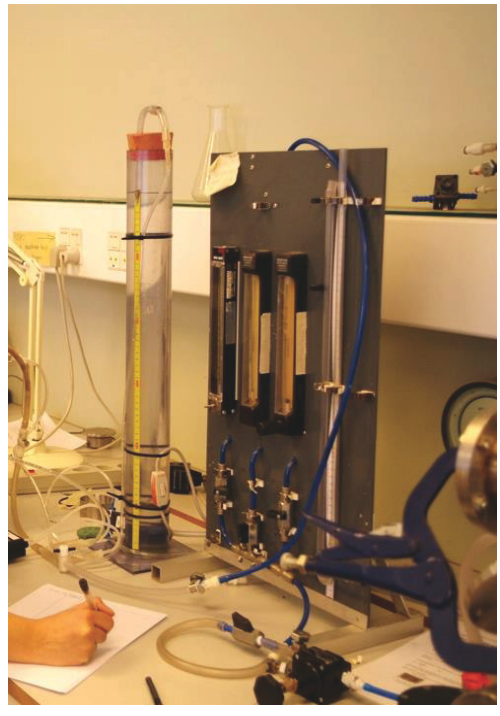

Figure 7. Air permeability measurement at the Department of Agroecology, Aarhus University (Paper I).

3.7 Bulk density and saturated hydraulic conductivity in small soil cores (Paper II)

Bulk density and saturated hydraulic conductivity (K_s) were measured on small soil cores (5 cm height, 7.2 cm diameter) taken from three depths (10, 30 and 50 cm) in all plots (1-8) at both sites (Upper, Lower). More details about the methods can be found in Paper II.

3.8 Water retention (Paper II)

Water retention was measured on small soil cores (5 cm height, 7.2 cm diameter) using the sand-box method (Eijkelkamp, model 102 08.01). From the water contents measured at saturation and at tensions of 10, 50 and 100 hPa, the volume of macropores (equivalent pore diameter >0.3 mm), large mesopores (0.3-0.06 mm) and small mesopores (0.06-0.03 mm) was obtained. Finally, the samples were oven-dried, and bulk density and volumetric water content at each tension step were calculated. More details about the methods can be found in Paper II.

3.9 Penetration resistance in the field (Paper II)

Soil penetration resistance was measured in the field using a hand-held Eijkelkamp penetrologger with a cone with 1 cm^2 base area and 60° apex angle. Measurements were made to 50 cm depth at 15 randomly selected locations per plot. A soil penetrometer measures the soil resistance to penetration, expressed as the force per unit cross-sectional area of the cone base (Bengough *et al*., 2001). The penetrometer is a useful tool for quickly evaluating the presence of compacted layers in the field (Minasny, 2012).

3.10 Dye tracing test in the field (Paper II)

For the dye tracing test, a 1 m^2 area in each plot was first irrigated with 20 L of water using a watering can. After 24 hours, 30 L of Brilliant Blue solution (4 g L-1) were applied. Three vertical soil profiles in each plot were then excavated to a depth of 150 cm, and the profile walls were carefully prepared with knives (see Figure 8 and Figure 9).

Figure 8. Excavation of dye tracing profiles during the dye tracing tests at the field sites.

Figure 9. Preparing profile walls for photographing dye pathways during the dye tracing test.

The plots were then photographed under both sunny and cloudy conditions, to provide different dye tracing images (see Figure 10 and Figure 11). At the Upper site, photographs taken from the soil surface down to 100 cm were analysed, whereas at the Lower site photographs taken from the soil surface down to only 70 cm depth were analysed, because of differences in groundwater levels at the two sites.

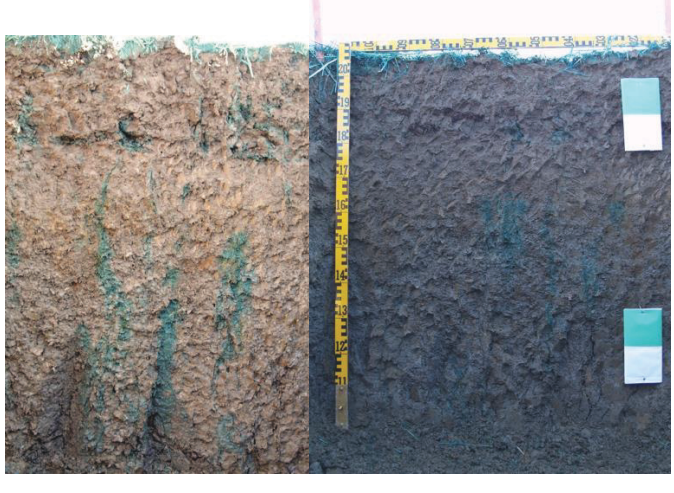

Figure 10. Example of dye tracing images taken under (left) sunny and (right) cloudy conditions.

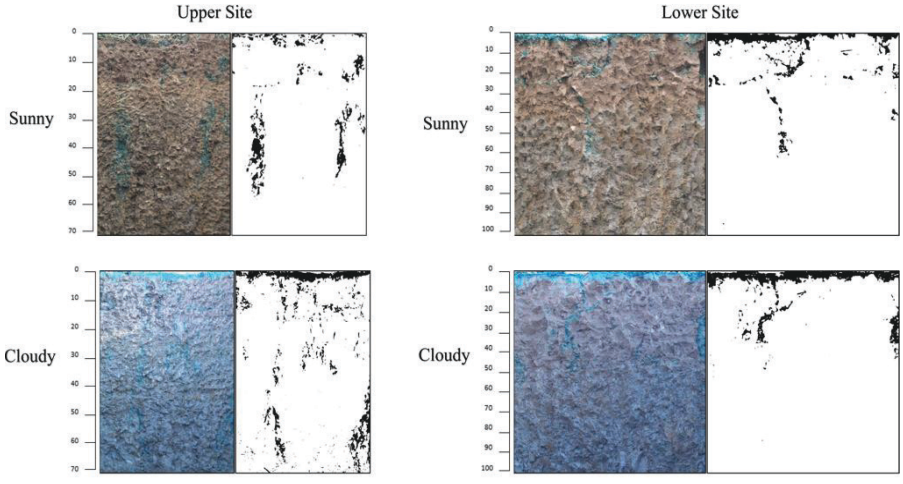

Figure 11. Examples of dye tracing images used for analysis of flow patterns at (left) the Upper site and (right) the Lower site under (top row) sunny and (bottom row) cloudy conditions.

Fraction of profile area dyed and number of stained flow paths were derived after image processing and calculation in Matlab. Full details of image processing and calculations can be found in Paper II.

3.11 Statistical analysis

4 Results and Discussion

This chapter presents selected results and discusses the main findings from Papers I and II. For a complete description of the results, see the relevant sections in Papers I and II.

4.1 Compaction effects on soil pore structure and transport properties

A summary of pore structure characteristics and transport properties (K_a, K_s and $t_{0.05}$) at the two sites is presented in Table 2. The table shows only data for 30 cm depth, because the compaction effects were most pronounced at this depth. Results from other depths studied and comparisons between these can be found in Paper II.

As can be seen in Table 2, macroporosity at the Lower site was in general smaller than at the Upper site. The compaction treatment caused a significant decrease (from 4.0% to 1%; p=0.03) in large mesopores (0.3-0.06 mm) at the Upper site. There was also a tendency for smaller percentages of pores ≥0.03 mm, large macropores ≥1.2 mm, small macropores ≥0.3 mm and number of pores (No.) in the compacted treatment compared with the control at the Upper site, although these differences were not significant. In contrast, only the number of pores decreased significantly at the Lower site (from 448.6 to 302.8; p=0.04) after compaction.

Compaction was found to significantly decrease both K_s and K_a at the Lower site, which is consistent with the decrease in the number of larger pores (Table 2). The 5% arrival time ($t_{0.05}$) was significantly higher in compacted plots than in control plots at the Lower site, suggesting less preferential flow transport after compaction at that site. At the Upper site, there was a tendency for lower K_s and K_a and higher $t_{0.05}$ in compacted plots, although these effects were not statistically significant. Higher values for $t_{0.05}$ after compaction were also

observed at the Upper site, suggesting that compaction decreased preferential flow/transport at both sites, but with much a stronger impact at the Lower site.

The differences between the two sites in their response to the applied compaction may be related to different pore volumes, as original macroporosity/mesoporosity was smaller at the Lower site than at the Upper site. Considering also the fact that the groundwater level was about 50 cm deeper at the Upper site than the Lower site, this suggests that the soil at the Upper site under grass ley (compared with cereal stubble at the Lower site) was drier at the time of compaction and probably more resistant to compaction.

Table 2. *Summary of pore size distribution, air permeability (K_a), saturated hydraulic conductivity (K_s), bulk density (Bd) and 5% arrival time ($t_{0.05}$) for soil at 30 cm depth at the Upper and Lower site. *p<0.05 (p-values calculated using log-transformed values for Ka and Ks)*

Site	Parameters	Sample size†	Control	Compacted	p-value
Upper	Porosity ≥0.03 mm	S	8.0%	4.0%	0.07
	Large macropores ≥1.2 mm	L	0.46%	0.35%	0.28
	Small macropores ≥0.3 mm	S	4.0%	2.0%	0.3
	Large mesopores (0.3-0.06 mm)	S	4.0%	1.0%	0.003*
	Small mesopores (0.06-0.03 mm)	S	1.0%	0.9%	0.1
	No. of pores ≥1.2 mm	L	642.3	518.7	0.37
	Bd (g cm $^{-3}$)	S	1.31	1.38	0.09
	Ka (µm^2)	L	33.5	21.0	0.14+
	Ks (cm h^{-1})	L	37.7	32.0	0.28+
	$t_{0.05}$ (-)	L	0.14	0.16	0.66
	Porosity ≥0.03 mm	S	1.0%	1.0%	0.82
Lower	Large macroporosity ≥1.2 mm	L	0.16%	0.09%	0.10
	Small macroporosity ≥0.3 mm	S	0.1%	0%	0.52
	Large mesopores (0.3-0.06 mm)	S	1.0%	1.0%	0.84
	Small mesopores (0.06-0.03 mm)	S	0.3%	0.8%	0.04*
	No. of pores ≥1.2 mm	L	448.6	302.8	0.004*
	Bd (g cm $^{-3}$)	S	1.37	1.46	0.08
	Ka (µm^2)	L	12.1	4.0	0.02*
	Ks (cm h^{-1})	L	10.9	0.09	0.05*
	$t_{0.05}$ (-)	L	0.13	0.25	0.02*

†L: Measurements on soil columns (20 cm height and 20 cm diameter) taken at 30-50 cm depth.

S: Measurements on small cores (5 cm height, 7.2 cm diameter) at 30 cm depth.

4.2 Relationship between soil pore structure and transport properties

Saturated hydraulic conductivity and air permeability were significantly correlated at both sites (Figure 12), as could be expected from a theoretical perspective (Ghanbarian *et al*., 2014).

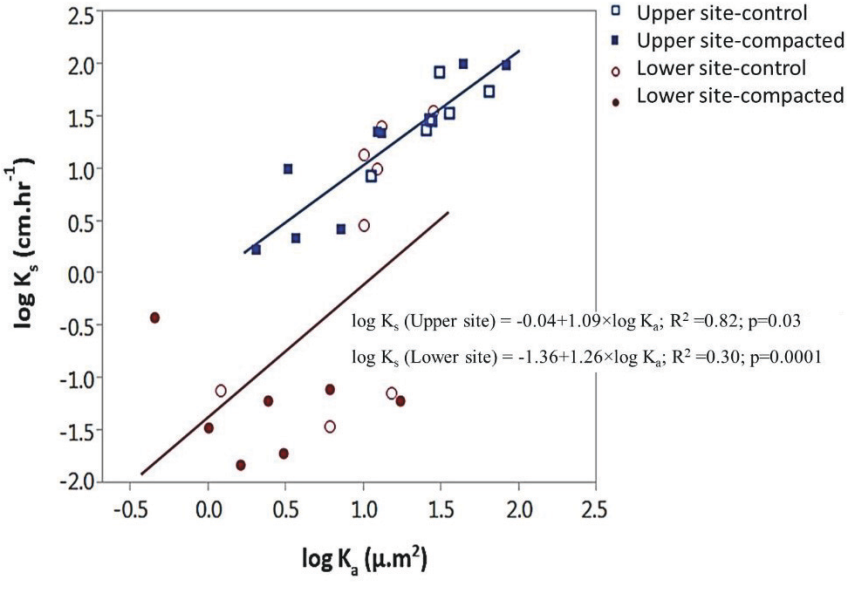

Figure 12. Relationship between air permeability (K_a) and saturated hydraulic conductivity (K_s) in soil from control and compacted plots at the Upper and Lower sites.

Saturated hydraulic conductivity was significantly correlated with large macropores ≥1.2 mm and decreased rapidly as the imaged macroporosity decreased from 0.3% towards zero, especially at Lower site (Figure 13). This means that water flow was strongly limited when the porosity was less than 0.3%. The correlation between K_s and connected porosity ≥1.2 mm is shown in Figure 14.

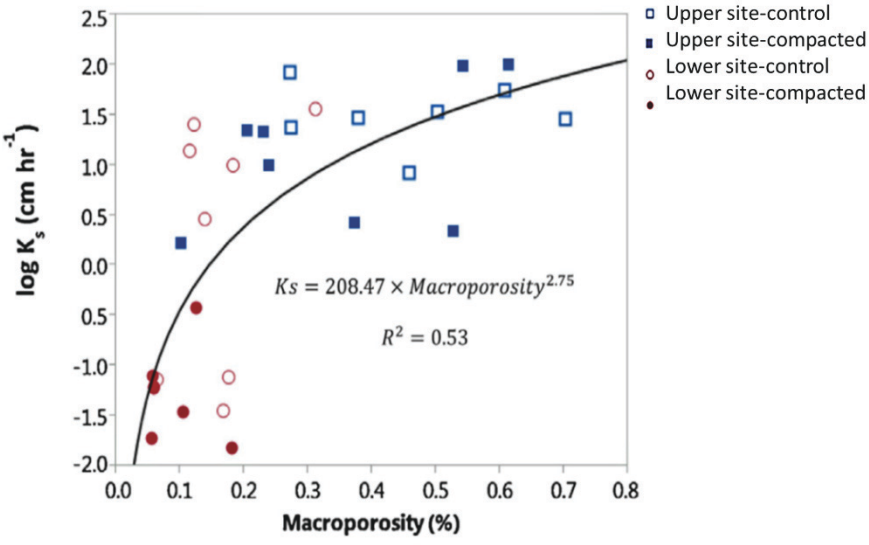

Figure 13. Relationship between saturated hydraulic conductivity (K_s) and percentage of macropores ≥1.2 mm determined from computed tomography (CT) images of large soil columns taken from control and compacted plots at the Upper and Lower sites..

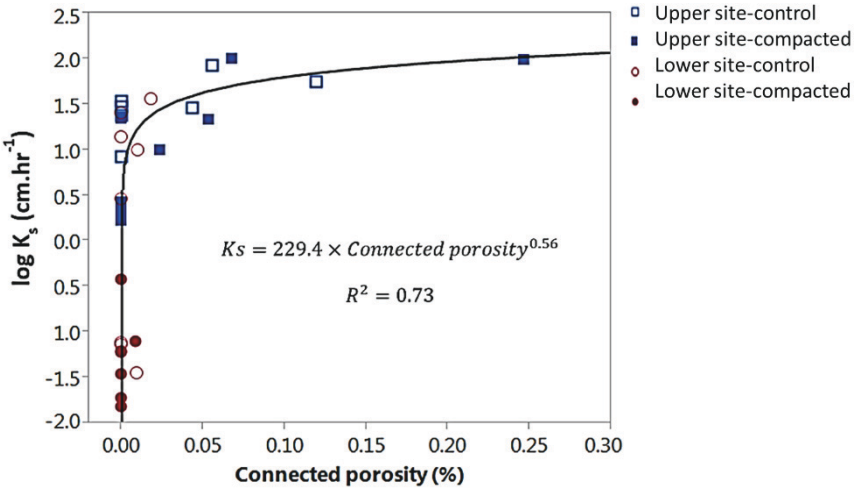

Figure 14. Relationship between saturated hydraulic conductivity (K_s) and percentage of connected pores determined from computed tomography (CT) images of large soil columns taken from control and compacted plots at the Upper and Lower sites.

The wide variation in K_s (from 0.06 to 34 cm hr^{-1}) observed in the large soil columns showed no association with connected porosity determined from CT images (Figure 14). Macroporosity in these columns varied from 0.18% to 0.5% (see Tables 2 and 3 in Paper I). It can be suggested that variation in K_s in these columns depended on connected porosity below the image resolution of X-ray CT (1.2 mm).

Data on K_s and porosity larger >0.03 mm measured on small soil cores (see Paper II for details) at both sites and all depths were used to check this suggestion. As shown in Figure 15, there was a linear relationship between logK_s and the volume of pores >0.03 mm in diameter. Comparing Figure 14 and Figure 15 suggests that transport functions were mostly governed by pores between 0.03-1.2 mm in diameter at both sites. This is an interesting finding, which may suggest that these pores (0.03-1.2 mm) are those most active in preferential flow/transport in this structured clay soil.

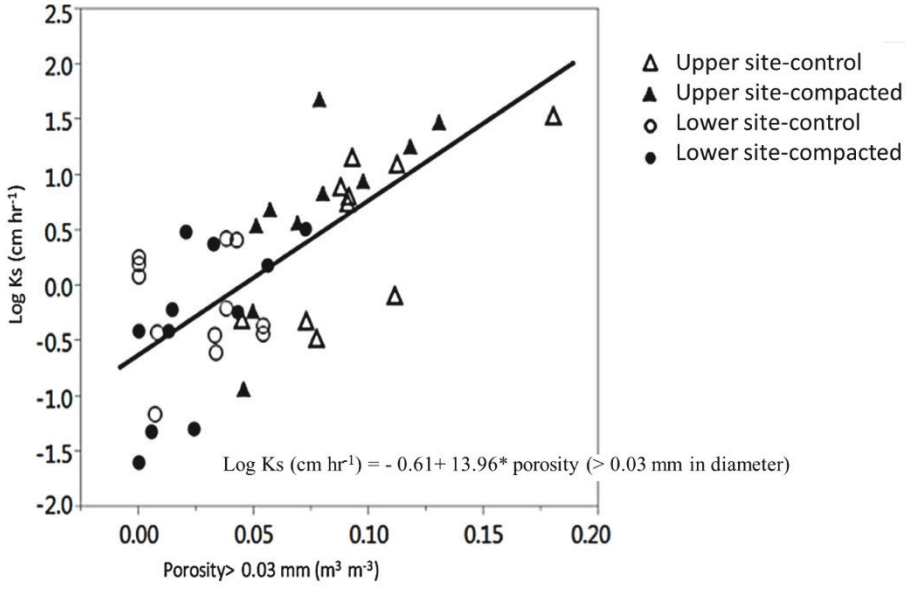

Figure 15. Saturated hydraulic conductivity (K_s) as a function of fraction of pores larger than 0.03 mm (corresponding to macropores, large mesopores and small mesopores) in soil from control and compacted plots at the Upper and Lower sites.

4.3 Compaction effects on preferential flow

The 5% arrival times for control plots at both sites were relatively small (0.14 at Upper site and 0.13 at Lower site), which according to Koestel *et al*. (2012)

indicates strong preferential flow. At the Lower site, compaction caused significant increases in $t_{0.05}$ (to 0.25), which means that compaction limited the strength of preferential flow at that site (Table 2). At the Upper site, no significant effect of compaction on preferential flow was found, although $t_{0.05}$ values were generally larger in the compacted treatment than control (mean 0.16 vs 0.14) (Table 2).

An inverse relationship between $t_{0.05}$ and macroporosity was found at the Lower site, whereas no trend was obvious at the Upper site (Figure 16). Loss of macroporosity due to compaction at the Lower site may have decreased preferential flow by reducing macropore continuity (Jarvis, 2007). This effect was apparent as the connected porosity was greater in control plots than in compacted plots at the Lower site (see Table 2 in Paper I). It can be therefore concluded that the effect of compaction on preferential flow may be attributed partly to a reduction in the volume and continuity of macropores smaller than 1.2 mm in diameter, which was the resolution of the CT scanner used in the present work.

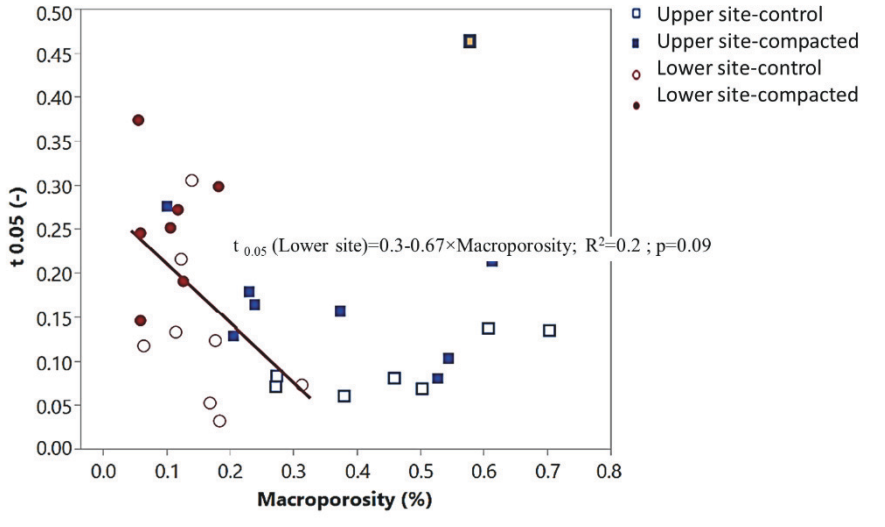

Figure 16. Relationship between 5% arrival time ($t_{0.05}$) and macroporosity in soil from control and compacted plots at the Upper and Lower sites. The high $t_{0.05}$ value for a control plot at the Upper site (square orange icon) was considered an outlier caused by an earthworm channel passing through the entire column, which resulted in rapid throughflow.

These results contradict those reported by Katuwal *et al*. (2015), who found a significant positive correlation between $t_{0.05}$ and macroporosity derived from CT images with similar image resolution as in this thesis. The samples analysed

in that study were taken from an agricultural field in Denmark with low (14.7-18.2%) clay content, whereas the samples analysed in this thesis had a much higher (45-54%) clay content. All samples analysed by Katuwal *et al*. (2015) had macroporosity greater than ~0.4%, while the columns studied in this thesis had much smaller values (see Tables 2 and 3 in Paper I). Larsbo *et al.* (2014) also found a higher degree of preferential flow (*i.e*. smaller $t_{0.05}$ values) in topsoil samples with lower CT image macroporosity and saturated hydraulic conductivity. In marked contrast to the narrow range of macroporosity (~0.1-0.5%) observed for soil columns in this thesis, macroporosity values in the soils studied by Larsbo *et al.* (2014) were higher and showed greater variation (range ~3 to 10%). Taken together, these findings suggest that, as hypothesised by Jarvis (2007), moderate compaction should increase the strength of preferential flow as macroporosity decreases but a few continuous macropores remain. As compaction becomes more severe, a critical point is reached at which pore continuity limits preferential flow. At this point, the saturated hydraulic conductivity of the soil may become so small that surface runoff may occur, depending on the surface boundary conditions in the field.

4.4 Dye patterns and penetration resistance one year after compaction

At both sites, penetration resistance increased markedly below 25 cm depth, indicating the presence of a compacted layer at this depth, even in the control treatment (Figure 17). The compaction treatment applied resulted in significantly higher penetration resistance (compared with the control) at 5-10 cm depth ($p=0.04$), 10-15 cm depth ($p=0.052$) and 15-20 cm depth ($p=0.05$) at the Lower site (Figure 17, right). In contrast, at the Upper site, penetration resistance was not significantly affected by compaction of the topsoil. The compacted plots at the Upper site tended to have higher penetrometer resistance in the subsoil (40-50 cm depth) (Figure 17, left), but these differences were not statistically significant ($p=0.09$ at 40-45 cm; $p=0.08$ at 45-50 cm).

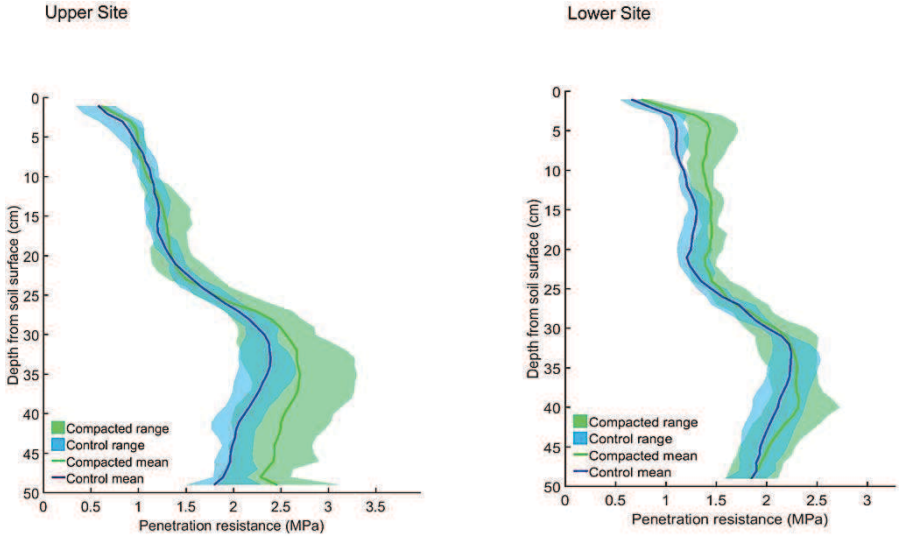

Figure 17. Penetration resistance patterns in soil at (left) the Upper site and (right) the Lower site before compaction (blue) and after compaction (green).

The results from the penetration resistance and dye tracing tests in the field suggest the presence of a compacted layer at about 20-30 cm depth at both sites (compare Figure 18 and Figure 17). The presence of this compacted layer was obvious at the Lower site from dye tracing, where the dyed area was mostly concentrated above 30 cm depth.

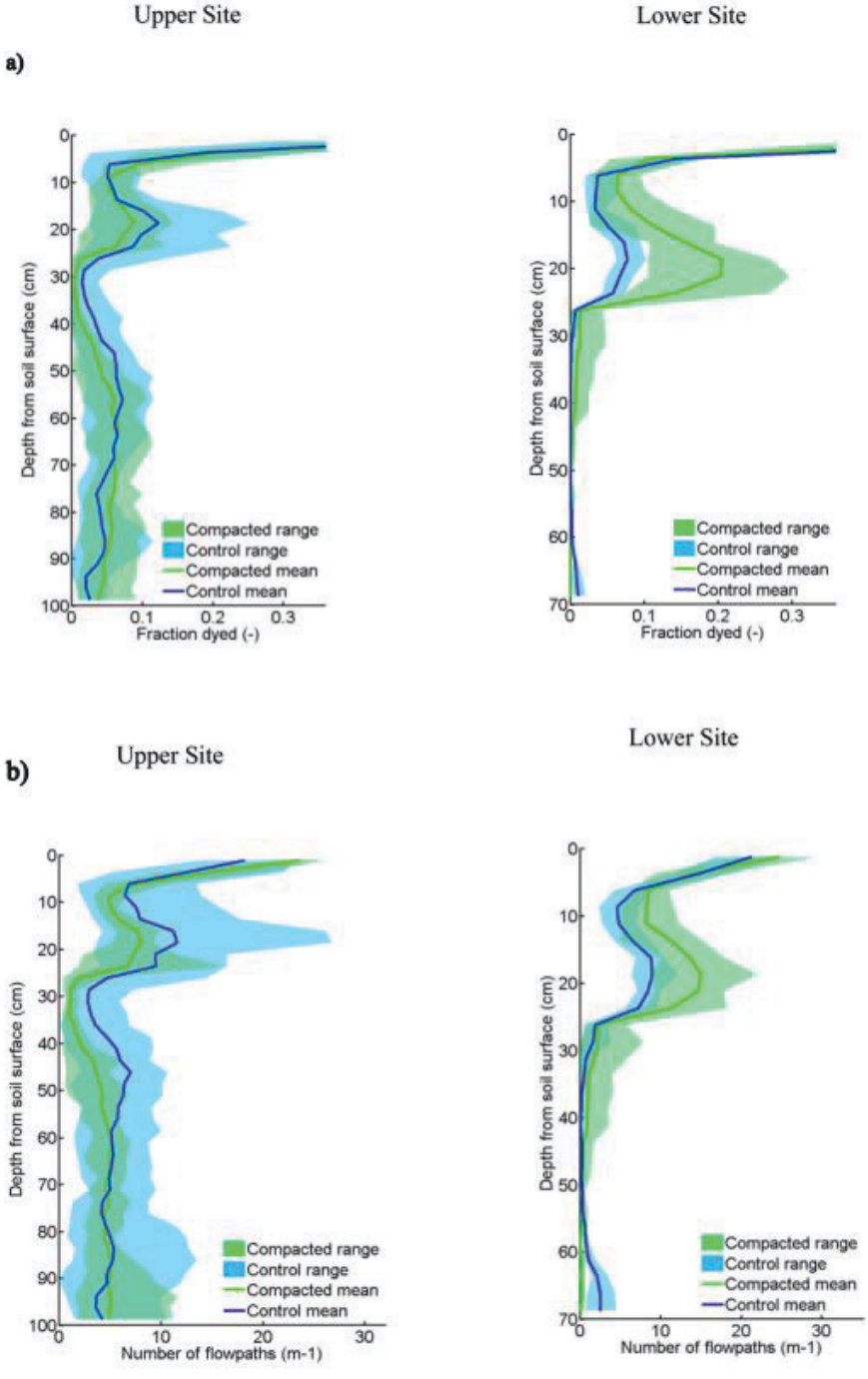

Figure 18. (a) Fraction of the soil profile dyed and (b) number of stained flow paths in control and compacted field soil at (left) the Upper site and (right) the Lower site.

Compaction led to a smaller dyed area (Figure 18a, left) and a smaller number of flow paths (Figure 18b, left) in the whole soil profile at the Upper site. At the Lower site, compaction resulted in a clear increase in the dyed area at 5-25 cm depth, with very little dyed area observed below 25 cm depth in both compacted and control plots at that site (Figure 18a, right). At the Lower site, ponding at the soil surface was observed during the dye tracing experiments, especially in the compacted plots, which supports the conclusion that water transport was limited due to the presence of a compacted layer (25 cm depth) characterised by greater penetration resistance. However, the ponding conditions at the Lower site did not induce any noticeable preferential transport of the dye solution deep into the subsoil (*Figure 19)*. This observation is consistent with our earlier findings for large columns (30-50 cm depth) taken at the Lower site, where almost no continuous macroporosity was found based on CT images (Mossadeghi-Björklund *et al*., 2016). However, the findings for the Lower site partly contradict those of Kulli *et al*. (2003), who reported larger dyed area in the subsoil because of compaction. They suggested that a decrease in permeability of the topsoil, caused by compaction, led to local ponding and enhanced preferential flow through remaining continuous macropores into the subsoil. Bogner *et al.* (2013) also found larger dyed area in the plough layer (25-30 cm depth) and concluded that flow transport above the plough layer was partly disconnected from the subsoil because of macropore disruption by tillage. However, in their study, preferential flow along cracks occurred in both compacted and control plots and the disconnected macropores below the plough layer still functioned as preferential flow paths (Bogner *et al*., 2013). This was not observed at the Lower site in this thesis, probably because there were not enough continuous macropores that could support preferential flow in the subsoil (Jarvis *et al*., 2016, 2017).

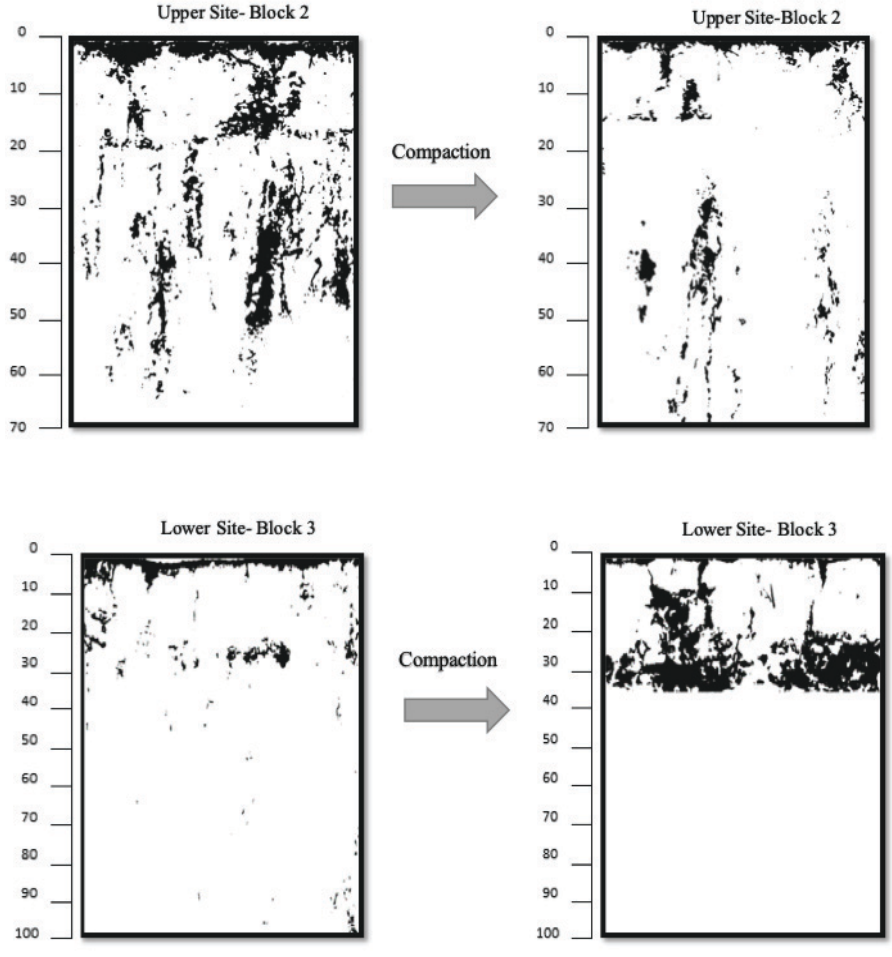

Figure 19. Examples of the effect of compaction on tracer dye flow pattern in soil in two treatment blocks at (top row) the Upper site and (bottom row) the Lower site.

An illustrative explanation of how compaction influenced flow transport at Upper site and Lower site is presented in Figure 20. As can be seen from the diagram, there was a clear decrease in preferential flow below the compacted layer (plough pan) in compacted plots, especially at the Lower site. This observation is consistent with our previous results for large soil columns (Mossadeghi-Björklund *et al.*, 2016), where compaction resulted in significantly higher $t_{0.05}$ (less preferential flow).

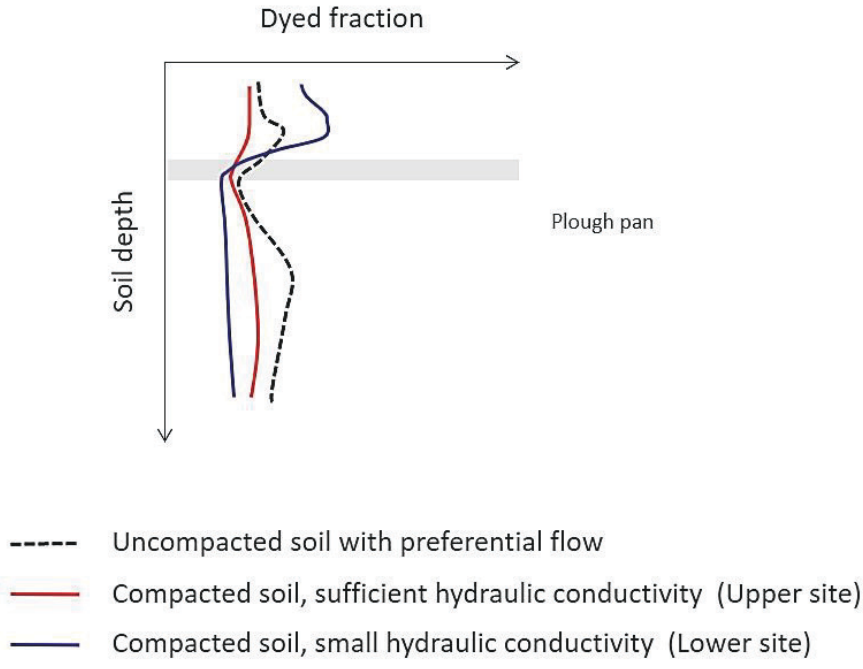

Figure 20. Illustration based on dye tracing images (*Figure 18*) of how compaction influenced flow paths in uncompacted and compacted soil at the Upper and Lower sites.

This reasoning is summarised in the conceptual model presented in Figure 21, which illustrates how preferential flow and surface runoff may be affected by compaction and natural regeneration of soil structural macropores (*e.g.* due to cracking or earthworm activity) following compaction. According to the model, moderate compaction may induce stronger preferential flow due to a decrease in near-saturated hydraulic conductivity and an increase in the size of the largest conducting pores (compared curve B with curve A in Figure 21). More severe compaction may result in an increased risk of surface runoff and weaker preferential flow, since the size of the largest pores in the soil is dramatically decreased (curve C in Figure 21). Larger soil macropores such as cracks and earthworm channels may subsequently regenerate, while the recovery of smaller pores affected by compaction is a slower process. This may lead to very strong preferential flow (curve D in Figure 21).

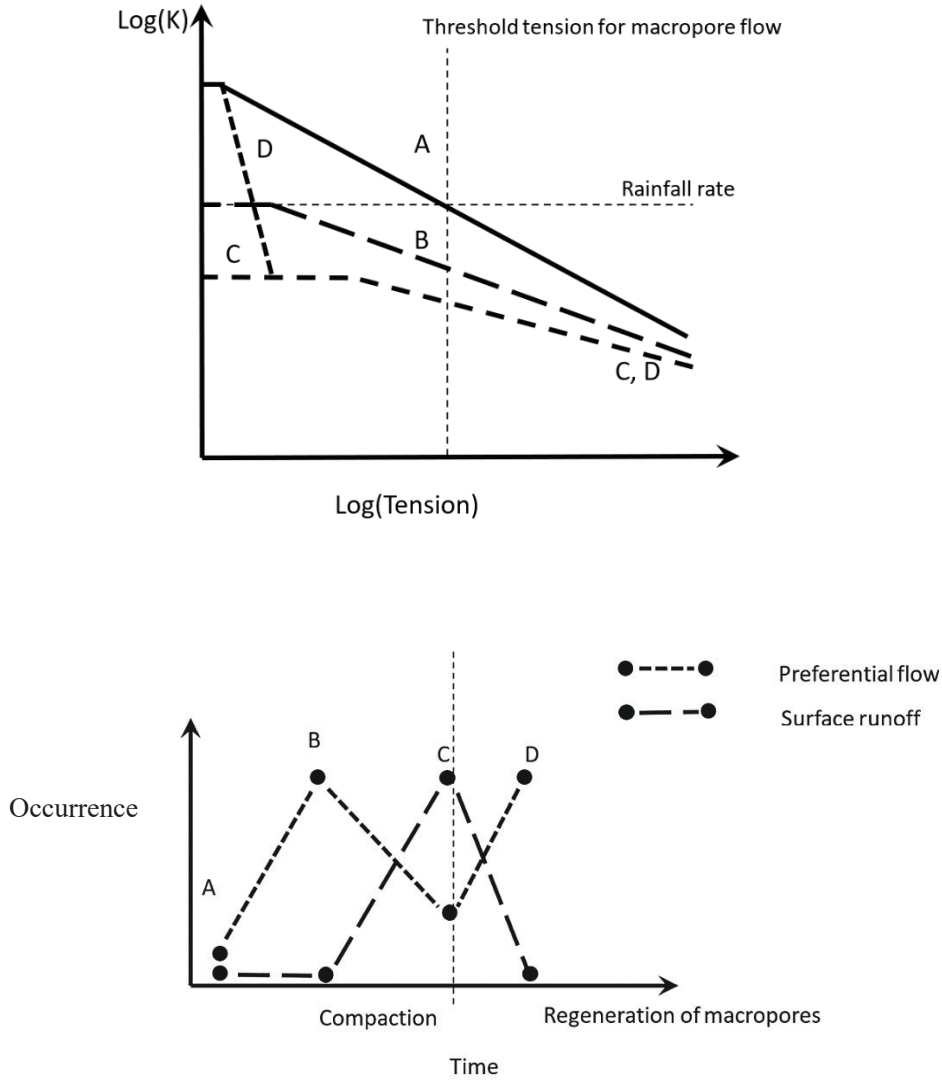

Figure 21. Conceptual model of preferential flow as influenced by soil compaction and subsequent recovery from compaction. A: no compaction, B: intermediate compaction, C: strong compaction, D: regeneration of macropores after compaction.

5 Conclusions

Significant effects of compaction on structural pore space (macroporosity) were found at 25-30 cm depth (compacted layer), with pronounced limitation of flow and transport below this depth. Both soils were ploughed after the compaction treatment, so the presence of a compacted layer indicates that ploughing did not remove the negative effects of compaction at 25-30 cm depth. Such subsoil compaction is an issue in many agricultural soils with a high clay content as it can lead to flood generation and runoff, a serious problem for farmers. This thesis showed that even quite small differences in initial soil and site conditions may significantly influence the extent to which applied compaction stresses affect the connectivity of structural pore space in soil and, consequently, water flow. To prevent subsoil compaction, it is important to consider soil conditions at the time of trafficking.

The neighbouring sites studied in this thesis had strong preferential flow in control plots. Water flow through preferential flow pathways can facilitate transport of fertilisers, pesticides, and contaminants to groundwater, causing harmful environmental problems. Since groundwater is used as drinking water, leaching of contaminants to groundwater may also affect human health.

Based on the results, a conceptual model was developed. It suggests that preferential flow is strongest at some intermediate level of compaction, at which macropore continuity is still maintained despite reductions in macroporosity. It also illustrates how compaction and subsequent recovery from compaction may affect soil susceptibility to preferential flow and surface runoff.

References

Alaoui, A., Goetz, B. (2008). Dye tracer and infiltration experiments to investigate macropore flow. *Geoderma* 144: 279-286.

Alaoui, A., Lipiec, J., Gerke, H.H. (2011). A review of the changes in the soil pore system due to deformation: A hydrodynamic perspective. *Soil Tillage Res*, 115-116: 1-15.

Allaire, S.E., Roulier, S., and Cessna, A.J. (2009). Quantifying preferential flow in soils: A review of different techniques. *J. Hydrol,* 378: 179– 204.

Arvidsson, J., Håkansson, I. (1996). Do effects of soil compaction persist after ploughing, Results from 21 long-term field experiments in Sweden. *Soil Tillage Res*, 39: 175-198.

Arvidsson, J. (1997). Soil compaction in agriculture- from soil stress to plant stress. Doctoral thesis. Department of soil and Environment, SLU. *Agraria* 41.

Bengough, A.G., Campbell, D.J., and O'Sullivan, M.F. (2001). Penetrometer techniques in relation to soil compaction and root growth. In Smith, K.A. and Mullins, C.E., Eds. *Soil and Environmental Analysis: Physical Methods*, 2nd ed., Marcel Dekker, New York, NY. pp. 377-403.

Bogner, C., Mirzaei. M., Ruy, S., Huwe, B. (2013). Microtopography, water storage and flow patterns in a fine-textured soil under agricultural use. *Hydrol. Process,* 27: 1797–1806.

Cassaro, F.A.M., Borkowski, A., Pires, L., Rosa, J., Saab, S. (2011). Characterization of a Brazilian clayey soil submitted to conventional and no-tillage management practices using pore size distribution analysis. *Soil Tillage Res,* 111: 175-179.

Chamen, W.C.T., Moxey, A.P., Towers, W., Balana, B., Hallet, P.D. t. (2015). Mitigating arable soil compaction: a review and analysis of available cost and benefit data. *Soil Tillage Res*, 146: 10-25.

Etana, A., Håkansson, I. (1994). Swedish experiments on the persistence of subsoil compaction caused by vehicles with high axle load. *Soil Tillage Res*, 29: 167-172.

Ghafoor, A., Jarvis, N.J., Stenström, J. (2013). Modelling pesticide sorption in the surface and subsurface soils of an agricultural catchment. *Pest Management Science*, 69: 919-929.

Ghanbarian, B., Hunt, A.G., Ewing, R.P., Skinner, T.E. (2014). Theoretical relationship between saturated hydraulic conductivity and air permeability under dry conditions: Continuum percolation theory. *Vadose Zone Journal*, 13: 1-6.

Goulding, K.W.T., Poulton, P.R., Webster, E.P., Howe, M.T. (2000). Nitrate leaching from the Broadbalk Wheat Experiment, Rothamsted, UK, as influenced by fertilizer and manure inputs and the weather. *Soil Use Manage*, 16: 244– 250.

Hendrickx, J.M.H., Flury, M. (2001). Uniform and preferential flow mechanisms in the vadose zone. In: *Conceptual models of flow and transport in the fractured vadose zone*. National academy press., Washington, D.C. pp.149-187.

Iversen, B.V., Moldrup, P., Schjonning, P., Loll, P. (2001). Air and water permeability in differently textured soils at two measurement scales. *Soil Science*, 166: 643-659.

Janssen, M., Lennartz, B. (2008). Characterization of preferential flow pathways through paddy bunds with dye tracer tests. *Soil Science Society of America Journal*, 72: 1756-1766.

Jarvis, N.J. (2007). A review of non-equilibrium water flow and solute transport in soil macropores: Principles, controlling factors and consequences for water quality. *European Journal of Soil Sciences*, 58: 523-546.

Jarvis, N., Koestel, J., Larsbo, M. (2016). Understanding preferential flow in the vadose zone: recent advances and future prospects. *Vadose Zone Journal*, 15 (12): 1-11.

Jury, W. A., Gardner, W. R., Gardner, W. H. (1991). *Soil physics: Water movement in soil*. fifth ed. John Willey & Sons, NY. pp.73-121.

Katuwal, S., Norgaard, T., Moldrup, P., Lamande, M., Wildenschild, D., de Jonge, L.W. (2015). Linking air and water transport in intact soils to macropore characteristics inferred from X-ray computed tomography. *Geoderma*, 237: 9-20.

Kim, H., Anderson, S.H., Motavalli, P.P., Gantzer, C.J. (2010). Compaction effects on soil macropore geometry and related parameters for an arable field. *Geoderma*, 160: 244-251.

Knudby, C., Carrera, J. (2005). On the relationship between indicators of geostatistical, flow and transport connectivity. *Advances in Water Resources,* 28: 405-421.

Koestel, J.K., Moeys, J., Jarvis, N.J. (2011). Evaluation of nonparametric shape measures for solute breakthrough curves. *Vadose Zone Journal*, 10: 1261-1275.

Koestel, J.K., Moeys, J., Jarvis, N.J. (2012). Meta-analysis of the effects of soil properties, site factors and experimental conditions on solute transport. *Hydrology and Earth System Sciences*, 16: 1647-1665.

Kulli, B., Gysi, M., Flühler, H. (2003). Visualizing soil compaction based on flow pattern analysis. *Soil and Tillage Research*, 70: 29-40.

Lamandé, M., Wildenschild, D., Berisso, F.E., Garbout, A., Marsh, M., Moldrup, P., Keller, T., Hansen, S.B., de Jonge, L.W., Schjonning, P. (2013). X-ray CT and Laboratory Measurements on Glacial Till Subsoil Cores: Assessment of Inherent and Compaction-Affected Soil Structure Characteristics. *Soil Sci*, 178: 359-368.

Larsbo, M., Koestel, J., Jarvis, N. (2014). Relations between macropore network characteristics and the degree of preferential solute transport. *Hydrology and Earth System Sciences*, 18: 5255-5269.

Lipiec, J., Håkansson, I. (2000). Influences of degree of compactness and matric water tension on some important plant growth factors. *Soil Tillage Res,* 53: 87-94.

Lipiec, J., Hatano, R. (2003). Quantification of compaction effects on soil physical properties and crop growth. *Geoderma*, 116: 107-136.

Minasny, B. (2012). Contrasting soil penetration resistance values acquired from dynamic and motor-operated penetrometers. *Geoderma*, 177: 57-62.

Mossadeghi-Björklund, M., Arvidsson, J., Keller, T., Koestel, J., Lamandé, M., Larsbo, M., Jarvis, N. (2016). Effects of subsoil compaction on hydraulic properties and preferential flow in a Swedish clay soil. *Soil Tillage Research*, 156: 91–98.

Mooney, SJ. (2002). Three-dimensional visualization and quantification of soil macroporosity and water flow patterns using computed tomography. *Soil Use & Manage*, 18: 142–151.

Petrovic, A.M., J.E. Siebert, and P.E. Rieke. (1982). Soil bulk density analysis in three dimensions by computed tomographic scanning. *Soil Sci. Soc. Am. J*, 46: 445–450.

Pires, L.F. (2011). Gamma-ray computed tomography to evaluate changes in the structure of a clayey soil due to agricultural traffic. Acta Scientiarum. *Agronomy*, 33: 411-416.

Schwen, A., Lawrence-Smith, G.H.-R.-E.J., Sinton, S.M., Carrick, S., Clothier, B.E., Buchan, G.D., Loiskandl, W. (2011). Hydraulic Properties and the Water-Conducting Porosity as Affected by Subsurface Compaction using Tension Infiltrometers. *Soil Sci. Soc. Am. J*, 75: 822-831.

Servadio, P., Marsili, A., Pagliai, M., Pellegrini, S., Vignozzi, N. (2001). Effects on some clay soil qualities following the passage of rubber-tracked and wheeled tractors in central Italy. *Soil and Tillage Research*, 61: 143-155.

Vanclooster, M., Mallants, D., Vanderborght, J., Diels, J., Van Orshoven, J., Feyen, J. (1995). Monitoring solute transport in a multi-layered sandy lysimeter using time domain reflectometry. *Soil Sci. Soc. Am. J*, 59: 337– 344

Wildenschild, D., Sheppard, A. P. (2013). X-ray imaging and analysis techniques for quantifying pore-scale structure and processes in subsurface porous medium systems. *Advances in Water Resources*. 51: 217-246.

Acknowledgements

I would like to thank my past main supervisor, the late Johan Arvidsson, who gave me the opportunity to start my research project and carry out my studies at SLU. I wish Johan were here today, he is greatly missed. My deepest thanks to my supervisor, Nick Jarvis, for all his valuable and scientific guidance, revisions and suggestions for improvements throughout my studies, especially during the publication of papers. I have learnt a lot from you, Nick, it was an honour to be your student. Special thanks to my present main supervisor, Thomas Keller, for all his guidance and useful discussions that helped me find my way, and also for his hospitality and our friendship. I would like to thank my co-supervisor Mats Larsbo for his guidance and tips and kindly providing Figures 17 and 18, and to John Koestel for his improving instructions during the breakthrough measurements. Many thanks to Johannes Forkman for excellent help with the statistics and for patiently listening and teaching me when I was lost handling my data. I thank Tomas Rydberg for his support when I was new at SLU and Ararso Etana for helping me in the field. Thanks to Per Schjønning, Mathieu Lamandé and the other nice people at Aarhus University in Denmark for letting me use their soil physics lab to perform some of my measurements. I am also grateful for the support I have received from my co-workers at the Department of Soil and Environment at SLU.

Last, but not least, I thank my parents, Ahmad-Ali Mossadeghi and Tooran Nazari, for letting their little bird find her own ways in life and for all their love. My sincere thanks go to my husband, Per Mossadeghi Björklund, for love, understanding and encouragement throughout this journey. Without your support I could not have managed it, Per. I am grateful to my lovely parents-in-law, Bertil and Monica Björklund, for their support during my studies. And I am so happy and proud to have two fantastic sons, Yosef and Yones Björklund, who understood when their mom needed to work long hours, thanks for giving me such energy and love, it kept me going.

Soil compaction caused by agricultural machinery is a major threat to soil functions. Compaction modifies soil pore structure, but it has been unknown how this affects the occurrence of preferential flow. Preferential water flow can facilitate transport of nutrients and pollutants adversely affecting groundwater quality. This thesis examined the impact of compaction on soil hydraulic properties and preferential water flow based on laboratory and in situ measurements. It was found that preferential flow is strongest at intermediate compaction levels.

Mona Mossadeghi Björklund
Department of Soil and Environment, SLU

SLU generates knowledge for the sustainable use of biological natural resources. Research, education, extension, as well as environmental monitoring and assessment are used to achieve this goal.

Online publication of the thesis summary: http://pub.epsilon.slu.se/

ISBN (print version) 978-91-7760-616-1
ISBN (electronic version) 978-91-7760-617-8